

# Direct Observation of Lateral Coupling Between Self-Assembled Quantum Dots

H. D. Robinson<sup>1</sup>, B. B. Goldberg<sup>1</sup>, J. L. Merz<sup>2</sup>

<sup>1</sup>*Dept. of Physics, Boston University, Boston MA 02215*

<sup>2</sup>*Dept. of Electrical Engineering, Notre Dame University, South Bend IN 46556*

(October 23, 2018)

## Abstract

Scattering of carriers between spatially separated zero dimensional states has been observed in a system of self-assembled  $\text{In}_{0.55}\text{Al}_{0.45}\text{As}$  quantum dots. We believe the interdot tunneling is mediated by localized states below the barrier band edge. The experiment was performed by taking photoluminescence excitation spectra at 4.2 K using a near-field scanning optical microscope. Surprisingly, the excitation spectrum from individual dots does not quench to zero at any energy, even when the energy of the exciting light is tuned below the barrier band edge. On top of this continuum, narrow resonances are observed in the emission lines of individual dots. These resonances tend to occur simultaneously in several emission lines, originating from different quantum dots, evincing interdot scattering.

Over the last few years, intense efforts have yielded a very detailed understanding of the physics of coupling between the electronic states of zero-dimensional (0D) quantum dots (QD) [1–5]. These processes are much less studied in 0D systems where the states are excitonic rather than electronic, and only one study [6], on a sample of cleaved edge overgrowth QDs, has reported a direct observation of coupling between individual QDs. In this Letter, we present the first such observation for the important case of self-assembled quantum dots (SADs) [7–10].

SADs form when an epitaxial layer of a semiconductor is grown on substrate with which it has a large lattice mismatch (Stranski-Krastanov growth mode) [11,12]. When grown beyond a critical thickness, the epitaxial layer spontaneously relieves the strain by forming 3D islands of relatively uniform size. The result is a layer of homogeneous, randomly distributed, high quality quantum dots connected by a thinner quantum well known as the wetting layer (WL). The growth method allows no control of dot positions, and the dot density is typically very high,  $\sim 10^{10} \text{ cm}^{-2}$ . Therefore, previous optical experiments have been largely limited to study low dot density samples in order to overcome the inevitable inhomogeneous broadening caused by studying a large ensemble of dots. In such systems, coupling between individual dots is unobservable. Using a near-field scanning optical microscope (NSOM) [13,14] operating at 4.2 K, we can study a small ensemble (10–25) of dots in samples where the dot density is sufficiently high for interdot coupling to occur.

The sample used consists of a  $\text{In}_{0.55}\text{Al}_{0.45}\text{As}$  quantum well, containing the dots, embedded in  $\text{Al}_{0.35}\text{Ga}_{0.65}\text{As}$  grown on a GaAs substrate, and has been studied extensively [15–18]. The dot density is known to be  $2 \times 10^{10} \text{ cm}^{-2}$ , the average lateral dot radius ( $R$ ) is 9 nm, and the ground state and the first excited state separation ( $\hbar\omega_{01}$ ) is approximately 40 meV.

Photoluminescence excitation (PLE) measurements were carried out in the near-field, illuminating the sample with the NSOM tip, and collecting the emission with conventional optics in the far-field. This arrangement produces the largest signal, but has in general a limited spatial resolution due to diffusion of carriers away from the tip. Here, however, the data has been gathered with the excitation energy below the wetting layer band edge,

where such diffusion is very small. The PLE excitation and detection regions are shown schematically in Fig. 1 on a photoluminescence spectrum of dots and the wetting layer exciton.

Fig. 2 shows the PLE spectra for two individual QD emission lines (sharp lines between 1840 meV and 1940 meV in Fig. 1) as the laser is tuned through the WL exciton. The spectra show two broad peaks which can be identified with the heavy-hole and light-hole excitons respectively. The most striking feature, however, is the fact that both lines remain non-zero even when the excitation energy is tuned to energies below the WL band-edge. This tail is present in the majority of emission lines that we have observed. As the excitation energy is decreased further, the signal intensity slowly decreases, typically by 10% to 25% every 10 meV.

When the laser is tuned more than 20 meV below the WL band-edge, another striking feature appears in the PLE spectra in the form of sharp resonances that begin to appear on top of the continuous background signal. Fig. 3a plots emission intensity as a function of both excitation (ordinate) and detection (abscissa) showing the QD emission lines (vertical dark lines) with a number of resonances (darker spots on the lines). The FWHM of typically 0.2–0.4 meV means the resonances originate from discrete QD states. While it is natural to assume these are the excited states of the individual quantum dots, one notices that resonances occur in several emission lines at the *exact* same excitation energy. This is illustrated in Fig. 3b by spectral line cuts at energies indicated by arrows in Fig. 3a.

We attribute the multiline resonances to a mechanism that allows excitons to scatter between discrete states in separate but nearby dots, giving rise to emission from the ground state of different dots at the same excitation energy. In order to arrive at this conclusion, we must first exclude several other possible explanations.

In several recent papers [19–21], emission from multiexciton states has been observed at high pump intensities. These states manifest themselves in the PL spectrum as several extra lines a few meV above and below the single exciton line. In NSOM experiments, the optical power density impacting on the very small area immediately underneath the tip

can typically reach the  $10^3$ – $10^4$  W/cm<sup>2</sup> range, making it quite reasonable to consider such non-linear effects.

In order to identify possible non-linearities, PL spectra were taken as a function of optical power. Two series of such spectra varying power over two orders of magnitude are shown in Fig. 4b and c. Note that intensities have been divided by incident power, so that linear power dependence appears as a constant shade of gray. Plainly, almost all observed emission lines scale linearly with power, both on and off resonance, except for a slight tendency to saturation at higher powers. When exciting above the WL band edge, non-linearities similar to what has been reported elsewhere [21] are observed in some emission lines. These lines disappear when tuning below the band-edge. We can therefore safely conclude that the various lines observed to resonate simultaneously are not due to different multiexciton states of the same dot. Also, the fact that the power dependence is linear on resonances means that the excitation and coupling processes themselves are linear, excluding for example two-photon or state-filling effects.

Previous work has shown there to be no perceptible phonon bottleneck [22] in SADs, leading to photoluminescence exclusively from the groundstate [23]. If the power of the pump light is high enough to cause state filling of the ground state, emission from higher lying states can occur [24]. Since it is clear from Fig. 4 that no significant saturation and therefore no state filling effects are observed, we can exclude the possibility of recombination from different excited states of the same dot as an explanation for the multiline resonances. Moreover, the separation between the multiresonance lines varies essentially randomly from 0.5 meV to over 25 meV. This is inconsistent both with the 40 meV excited state separation in this sample and any level splitting due for example to deviation from cylindrical symmetry in the dots, which reaches at most a few meV.

Having excluded non-linear effects and excited states of the same dot, we conclude that each line in a set of multiresonant lines originate from a separate quantum dot, and consequently there exists a mechanism for scattering excitons between dots. Indications of this type of behavior has been reported in SAD systems with much higher dot density [25], but

this experiment shows the first direct evidence of this effect.

In order to estimate the probability of direct dot-to-dot tunneling as a mechanism for interdot scattering we have carried out a simple Monte-Carlo simulation of the spatial dot distribution for the sample, assuming hard-wall potentials the size of the dots preventing overlap, but otherwise allowing equal probability for all dot separations. This random dot distribution is consistent with experimental observations. [8,26] We find that 70% of the time, the nearest neighbor edge-to-edge separation is larger than 10 nm (86% for 5 nm).

The tunneling time can be estimated in the small coupling limit to be  $\tau = \frac{\hbar}{2\alpha}$ , where  $\alpha = \int \varphi_0(\mathbf{r})V_0(\mathbf{r})\varphi_1(\mathbf{r})d\mathbf{r}$ . By taking the potential

$$V(\mathbf{r}) = \begin{cases} \frac{1}{2}m\omega_{01}^2(r^2 - R^2) & r < R \\ 0 & R > r \end{cases}$$

and the wavefunction  $\varphi(\mathbf{r})$  to be the solution to the harmonic oscillator for  $r < R$  and the appropriate combination of Bessel functions  $K_0$  and  $K_2$  for  $r > R$ , we can estimate  $\tau$  for tunneling between second excited states. We have used  $m = 0.2$ ,  $R = 9$  nm, and  $\hbar\omega_{01} = 37$  meV, which are close to the measured values, and yields a confinement of 130 meV, consistent with the measured distance between WL and QD emission. We find  $\tau = 1$  ns for a 10 nm dot separation, which is of the same order as the exciton recombination time. This would mean that by our estimate about 30% of the dots can be involved in interdot tunneling, which is consistent with the data. However, if the energy difference between initial and final states is large compared to their widths, which is almost always the case, the tunneling must be assisted by emission or absorption of a LA phonon in order to conserve energy. This will make the process orders of magnitude slower, implying that direct tunneling between dots is probably too weak to fully explain what we have observed.

The simplest way to explain the observations without invoking direct tunneling would be to place localized states inside the barrier between the dots. If the density of such states is high enough, they can act as intermediate states for carriers moving between dots. This would also explain why the signal remains finite when exciting below the WL band edge, as

the states form a “tail” in the density of states inside the bandgap, analogous to the situation in glasses. In a two dimensional system, any type of disorder, e.g. interface roughness and alloy fluctuations, will give rise to localized states. Such disorder is certainly present, and if it is severe enough, states in the WL may localize on a length scale small enough for this explanation to apply.

Experimental evidence supports this hypothesis. Firstly, In PL, the peak associated with the wetting layer exciton is unusually wide, and has a fair amount of structure in the near-field. An example of this is shown in Fig. 1. This could be taken as an indication of the non-2D nature of the WL. Secondly, as can be seen in Fig. 5, a close examination of PL spectra at energies immediately below the WL exciton peak reveals a multitude of very weak, narrow lines, the brightest of which show strong saturation at high excitation powers. This is a clear indication of the presence of localized states.

Since the observed resonances are consistent with scattering from the second excited state of the dots, no resonances being observed at higher or lower energies, and since the peaks observed between WL and QD emissions are so weak and easy to saturate, we can conclude that we are indeed observing scattering from one dot to another, rather than from one WL state into several nearby dots.

We finally note two possible consequences of our observations for the physics of SAD systems, both due to new carrier relaxation channels being opened by interdot coupling. We have already noted that SADs display no phonon bottleneck, and several explanations for this have been suggested, including multiphonon emission [27–29] and scattering off of holes [30] or deep-level impurities [31]. It is possible that interdot scattering provides an additional explanation for this, which moreover sets SADs apart from related 0D systems where a phonon bottleneck has been observed [32]. Another possible consequence is that state-filling at high optical powers may be more difficult to observe. Indeed, far-field experiments at much higher powers than used in the near-field show no emission from higher excited states, and we tentatively suggest this as a method, not involving high spatial resolution techniques, for testing the strength of lateral interdot coupling in self-assembled quantum dot systems.

This work was supported by NSF Grant No. DMR-9701958. The authors gratefully acknowledge P. M. Petroff, whose laboratory produced the sample used for these studies. The authors also thank Pawel Hawrylak for helpful discussions.

## REFERENCES

- [1] G. Klimeck, G. Chen, and S. Datta, Phys. Rev. B **50**, 2316 (1994).
- [2] N. C. van der Vaart, S. F. Godijn, Y. N. Nazarov, C. J. P. M. Harmans, and J. E. Mooij, Phys. Rev. Lett. **74**, 4702 (1995).
- [3] R. H. Blick, R. J. Haug, J. Weis, D. D. Pfannkuche, K. v. Klitzing, and K. Eberl, Phys. Rev. B **53**, 7899 (1996).
- [4] T. Schmidt, R. J. Haug, K. v. Klitzing, A. Förster, and H. Lüth, Phys. Rev. Lett. **78**, 1544 (1997).
- [5] T. H. Oosterkamp, S. F. Godjin, M. J. Uilenreef, Y. V. Nazarov, N. C. van der Vaart, and L. P. Kouwenhoven, Phys. Rev. Lett. **80**, 4951 (1998).
- [6] G. Schedelbeck, W. Wegscheider, M. Bichler, and G. Abstreiter, Science **278**, 1792 (1997).
- [7] P. M. Petroff and S. P. Denbaars, Superlatt. Microstruct. **15**, 15 (1994).
- [8] J. M. Moison, F. Houzay, L. Leprince, E. André, and O. Vatel, Appl. Phys. Lett **64**, 196 (1994).
- [9] J.-Y. Marzin, J.-M. Gérard, A. Israël, D. Barrier, and G. Bastard, Phys. Rev. Lett. **73**, 716 (1994).
- [10] M. Grundmann, N. N. Ledentsov, R. Heitz, L. Eckey, J. Böhrer, D. Bimberg, S. S. Ruminov, P. Werner, U. Richter, J. Heydenreich, V. M. Ustinov, A. Y. Egorov, A. E. Zhukov, P. S. Kop'ev, and Z. I. Alferov, Phys. Status Solidi B **188**, 249 (1995).
- [11] I. N. Stranski and L. V. Krastanow, Akad. Wiss. Lit. Mainz Math.-Natur. Kl. IIb **146**, 797 (1939).
- [12] L. Goldstein, F. Glas, J.-Y. Marzin, M. N. Charasse, and G. L. Roux, Appl. Phys. Lett. **47**, 1099 (1985).

- [13] E. Betzig and J. K. Trautman, *Science* **257**, 189 (1992).
- [14] M. A. Paesler and P. J. Moyer, *Near-Field Optics: Instrumentation & Applications* (John Wiley & Sons, New York, 1996).
- [15] S. Fafard, R. Leon, J. L. Merz, and P. M. Petroff, *Phys. Rev. B* **52**, 5752 (1995).
- [16] R. Leon, S. Fafard, D. Leonard, J. L. Merz, and P. M. Petroff, *Science* **267**, 1966 (1995).
- [17] R. Leon, S. Fafard, D. Leonard, J. L. Merz, and P. M. Petroff, *Appl. Phys. Lett.* **67**, 521 (1995).
- [18] P. D. Wang, J. L. Merz, S. Fafard, R. Leon, D. Leonard, G. Medeiros-Ribeiro, M. Oestrich, P. M. Petroff, K. Uchida, N. Miura, H. Akiyama, and H. Sakaki, *Phys. Rev. B* **53**, 16458 (1995).
- [19] L. Landin, M. S. Miller, M.-E. Pistol, C. E. Pryor, and L. Samuelson, *Science* **280**, 262 (1998).
- [20] E. Dekel, D. Gershoni, E. Ehrenfreund, D. Spektor, J. M. Garcia, and P. M. Petroff, *Phys. Rev. Lett.* **80**, 4991 (1998).
- [21] A. Chavez-Perez, J. Temmyo, H. Kamada, H. Gotoh, and H. Ando, *Appl. Phys. Lett.* **72**, 3494 (1998).
- [22] U. Bockelmann and G. Bastard, *Phys. Rev. B* **42**, 8947 (1990).
- [23] G. Wang, S. Fafard, D. Leonard, J. E. Bowers, and J. L. M. an P. M. Petroff, *Appl. Phys. Lett.* **64**, 2815 (1994).
- [24] S. Raymond, S. Fafard, P. J. Poole, A. Wojs, P. Hawrylak, S. Charbonneau, D. Leonard, R. Leon, P. M. Petroff, and J. L. Merz, *Phys. Rev. B* **54**, 11548 (1996).
- [25] D. L. Huffaker, L. A. Graham, and D. G. Deppe, *Appl. Phys. Lett.* **72**, 214 (1998).
- [26] D. Leonard, S. Fafard, K. Pond, Y. H. Zhang, J. L. Merz, and P. M. Petroff, *J. Vac.*

Sci. Technol. B **12**, 2516 (1994).

[27] T. Inoshita and H. Sakaki, Phys. Rev. B **46**, 7260 (1992).

[28] B. Ohnesorge, M. Albrecht, J. Oshinowo, A. Forchel, and Y. Arakawa, Phys. Rev. B **54**, 11532 (1996).

[29] R. Heitz, M. Veit, N. N. Ledentsov, A. Hoffmann, D. Bimberg, V. M. Ustinov, P. S. Kop'ev, and Z. I. Alferov, Phys. Rev. B **56**, 10435 (1997).

[30] T. S. Sosnowski, T. B. Norris, H. Jiang, J. Singh, K. Kamath, and P. Bhattacharya, Phys. Rev. B Rapid Commun. **57**, R9423 (1998).

[31] P. C. Sercel, Phys. Rev. B **51**, 14532 (1995).

[32] J. Hasen, L. N. Pfeiffer, A. Pinczuk, S. He, K. W. West, and B. S. Dennis, Nature **390**, 54 (1997).

## FIGURES

FIG. 1. A typical photoluminescence spectrum in the near-field, where emission lines from individual quantum dots can be resolved. Detection and excitation regions for collecting PLE data are schematically indicated. The feature around 1995 meV is the wetting layer exciton.

FIG. 2. A comparison of the PLE of two quantum dot emission lines with the PL of the wetting layer exciton. There are no vertical offsets of the graphs.

FIG. 3. (a) Typical plot of intensity vs. laser- and detection-energy. Numerous resonances are visible. The arrows mark vertical line cuts shown in (b). (b) Line cuts from a, offset vertically for clarity.

FIG. 4. (a) PLE of strong multiline resonance. Arrows indicate excitation energies for power dependence off resonance, shown in (b), and on resonance, shown in (c).

FIG. 5. PL with  $\lambda_{exc} = 514.5$  nm. The spectra have been scaled inversely to power and offset slightly to enable mutual comparison. The heights of the WL exciton peaks at 1995 meV are about eight times the full vertical scale of the figure.

Figure 1

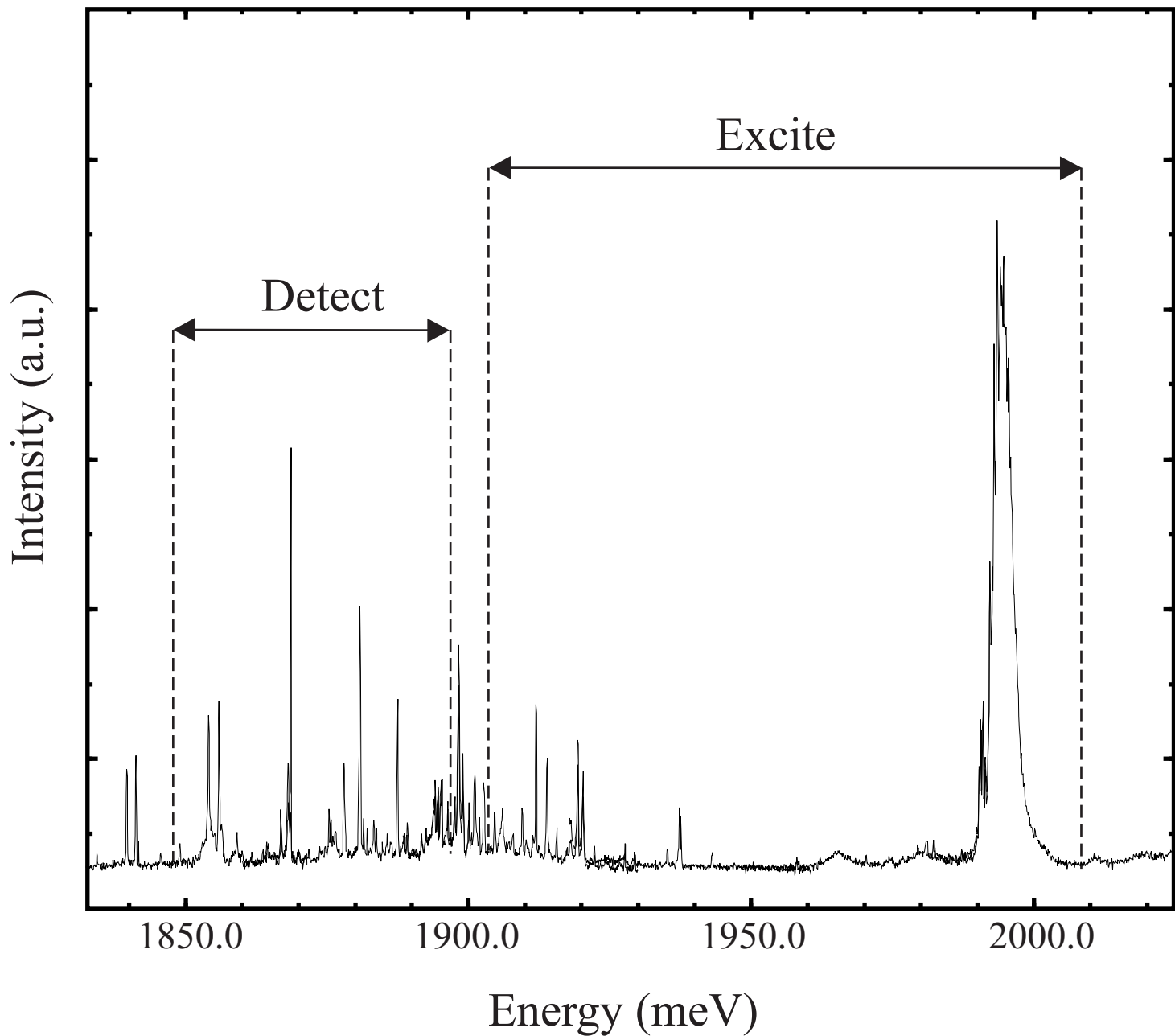
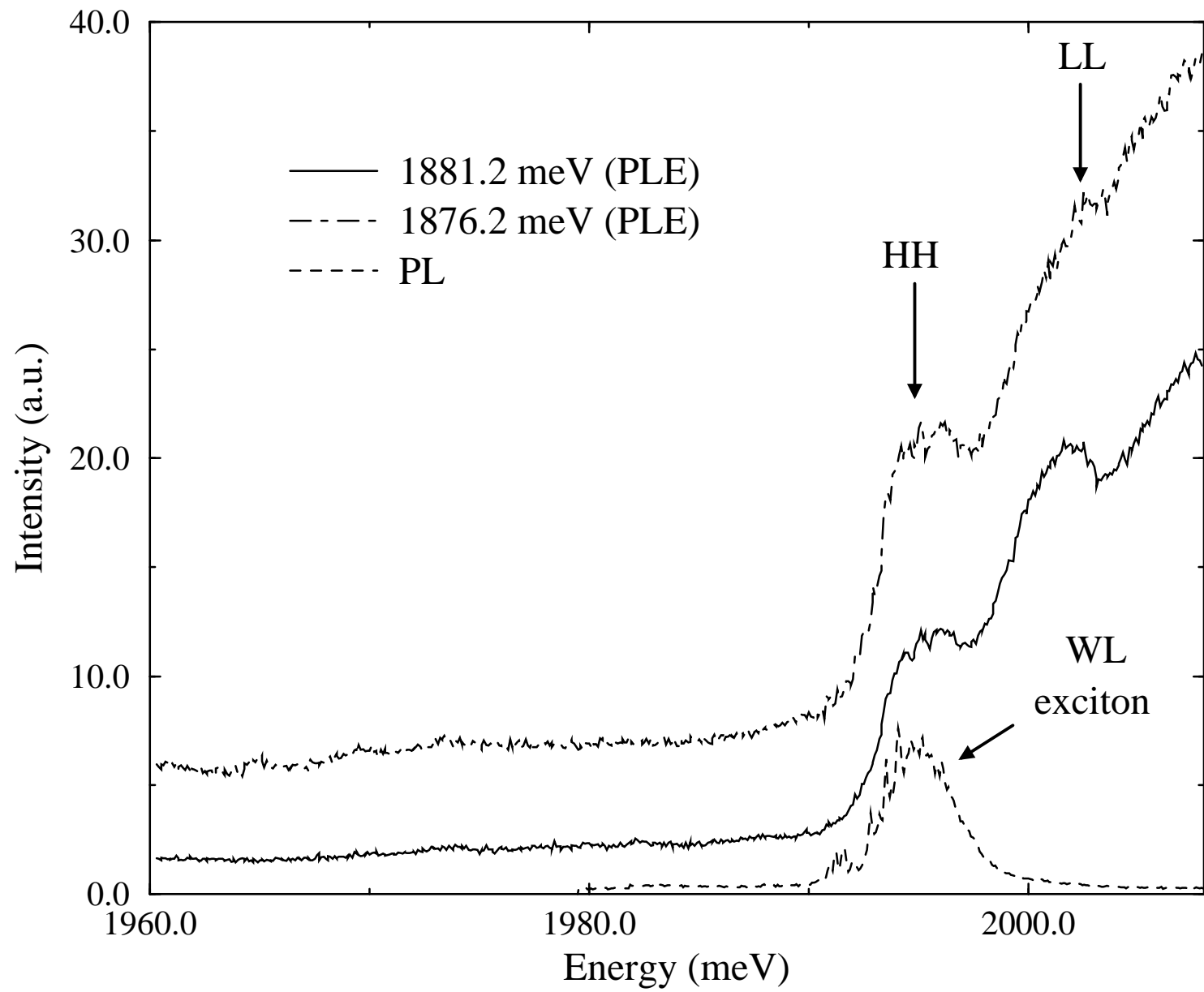


Figure 2



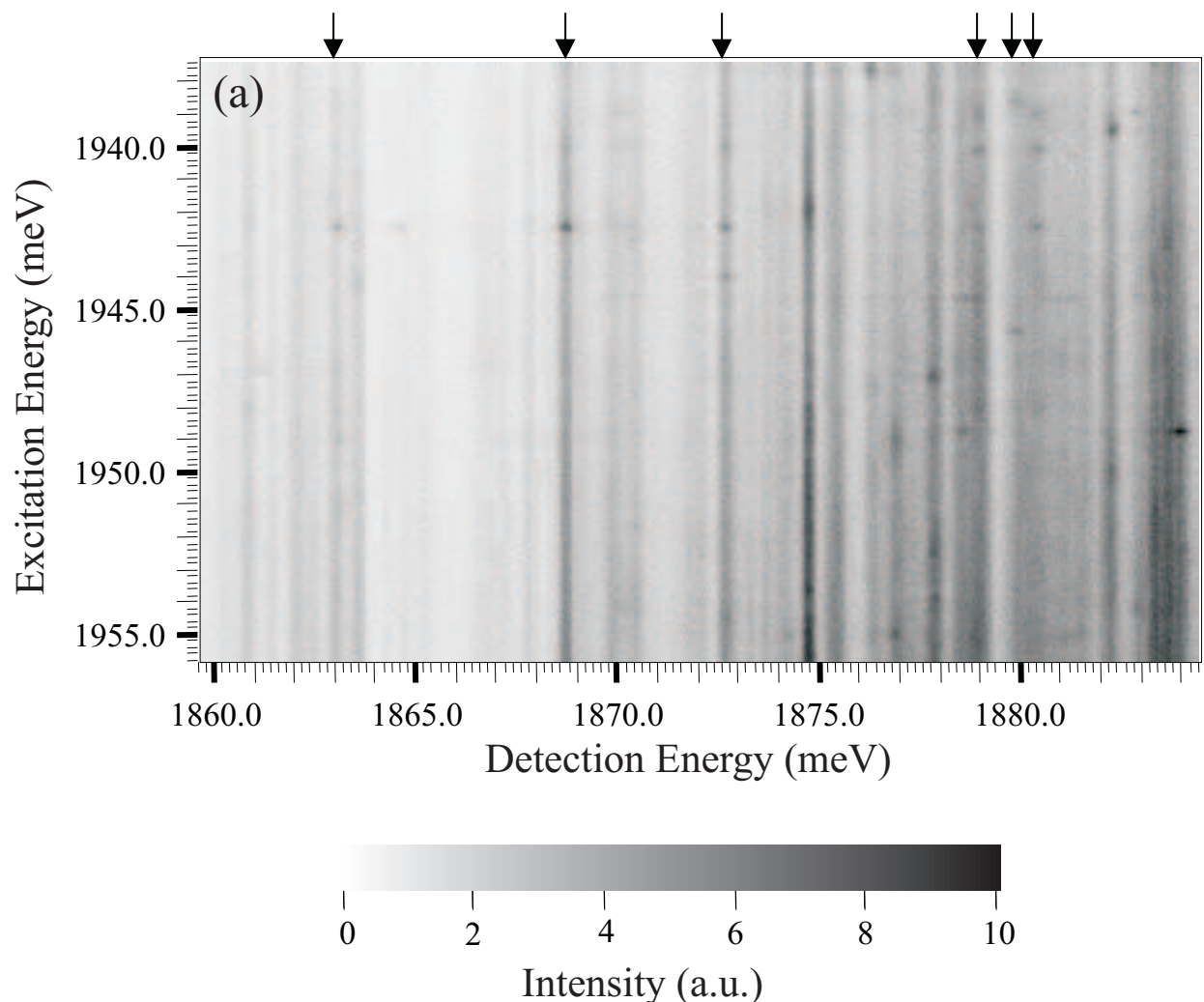
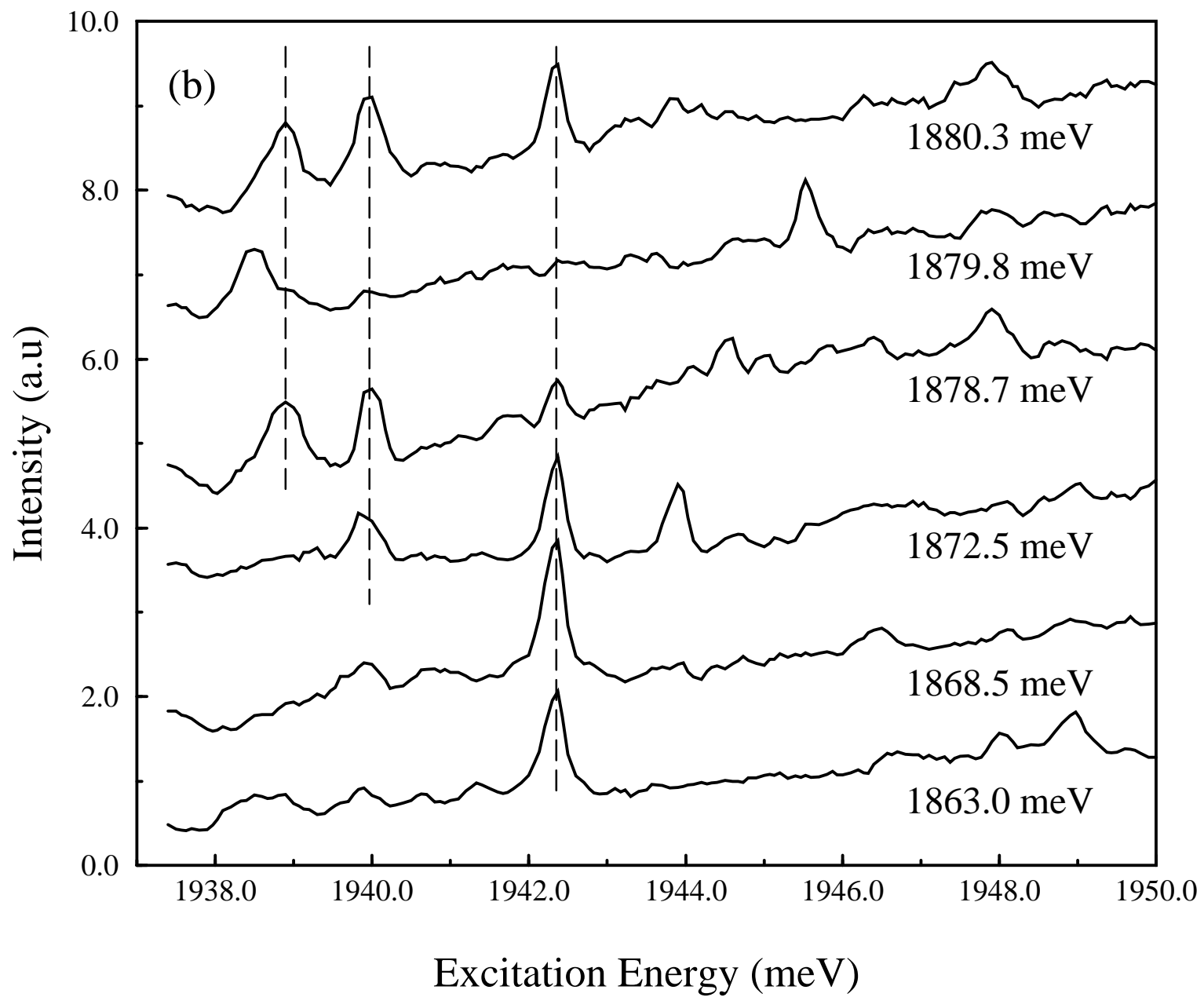


Figure 3a

Figure 3b



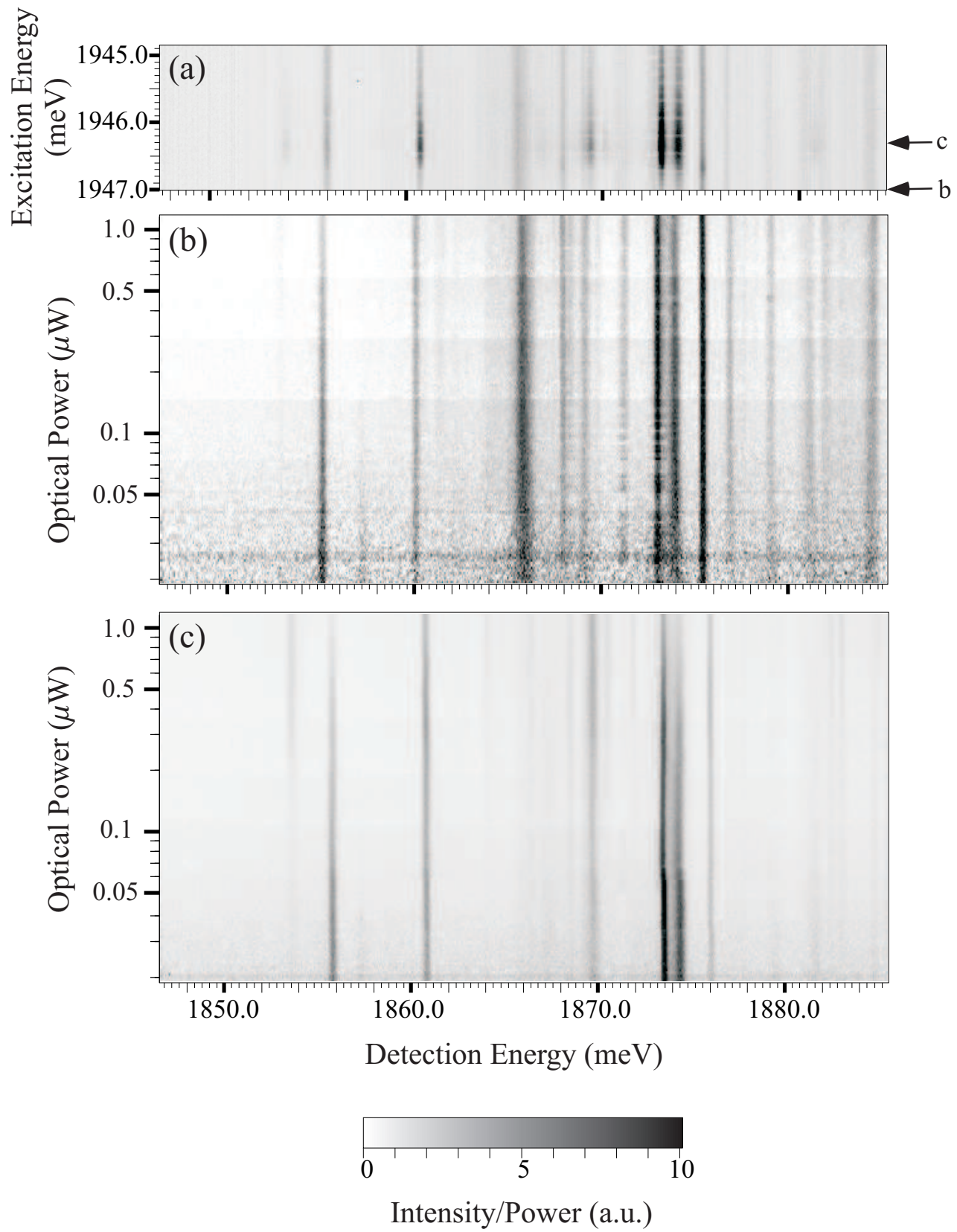


Figure 4

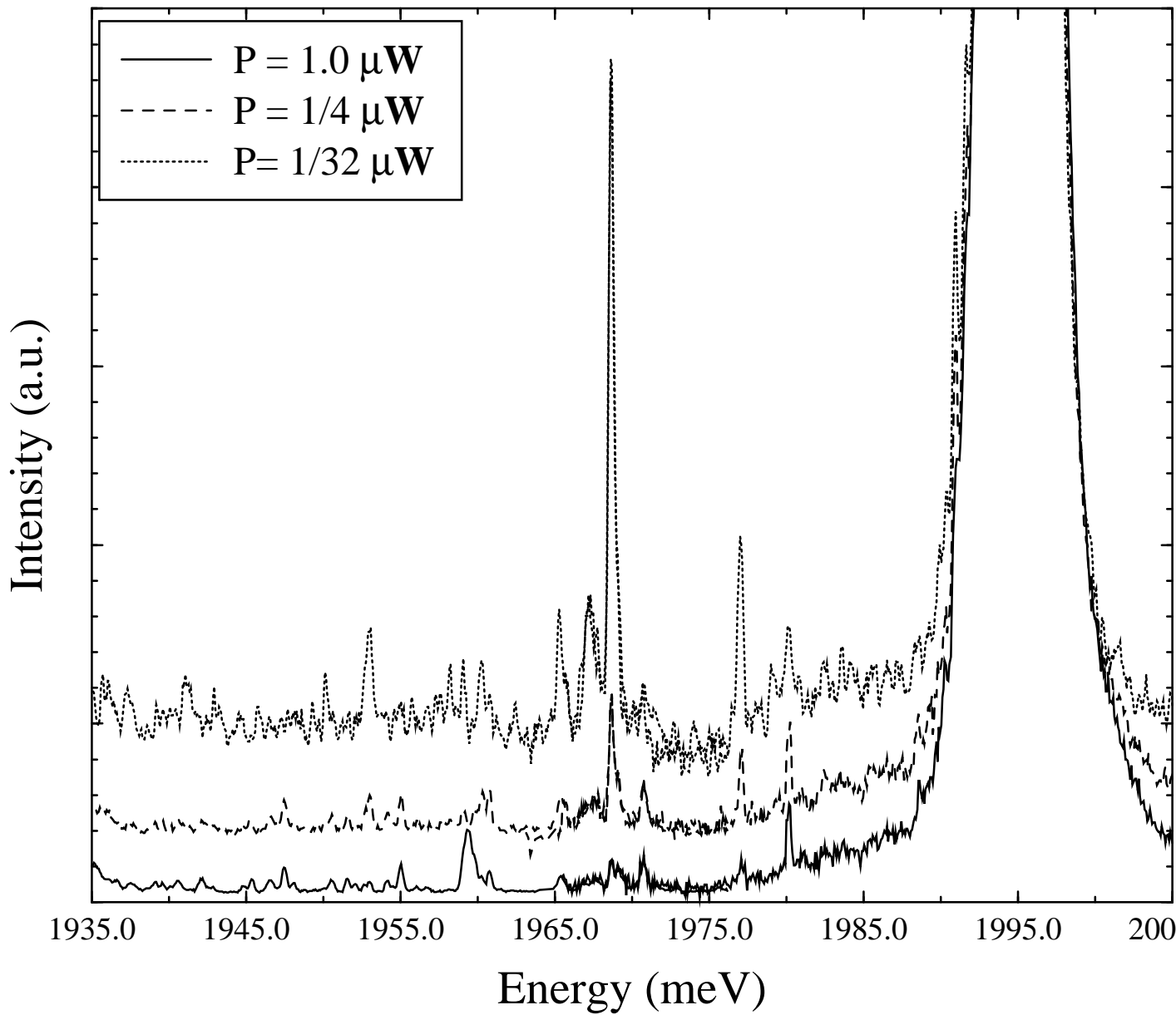


Figure 5